Investigation of the Radical Product Channel of the $CH_3OCH_2O_2 + HO_2$ Reaction in the Gas Phase

M. E. Jenkin,*,† M. D. Hurley,‡ and T. J. Wallington‡

Atmospheric Chemistry Services, Okehampton, Devon, EX20 1FB, U.K., and Research and Advanced Engineering, Ford Motor Company, SRL-3083, PO Box 2053, Dearborn, Michigan 48121-2053

Received: August 24, 2009; Revised Manuscript Received: October 16, 2009

The reaction of $CH_3OCH_2O_2$ with HO_2 has been investigated at 296 K and 700 Torr using long path FTIR spectroscopy, during photolysis of $Cl_2/CH_3OCH_3/CH_3OH$/air mixtures. The branching ratio for the reaction channel forming CH_3OCH_2O, OH, and O_2 has been determined from experiments in which OH radicals were scavenged by addition of benzene to the system, with subsequent formation of phenol used as the primary diagnostic for OH radical formation. The dependence of the phenol yield on the initial peroxy radical precursor reagent concentration ratio, $[CH_3OH]_0/[CH_3OCH_3]_0$, is consistent with prompt OH formation resulting mainly from the reaction of $CH_3OCH_2O_2$ with HO_2, such that the inferred prompt yield of OH is well-correlated with that of CH_3OCH_2OOH, a well-established product of the $CH_3OCH_2O_2 + HO_2$ reaction. The system was fully characterized by simulation, using a detailed chemical mechanism which included other established sources of OH in the system. This allowed a branching ratio of $k_{2c}/k_2 = 0.19 \pm 0.08$ to be determined. The results therefore provide strong indirect evidence for the participation of the radical-forming channel of the title reaction.

1. Introduction

The reactions of organic peroxy radicals (RO_2) with the hydroperoxy radical (HO_2) have long been considered as chain terminating reactions that make an important contribution to controlling the concentrations of free radicals under atmospheric conditions, particularly when the availability of nitrogen oxides (NO_X) is limited.[1−4] Whereas radical termination via the near-exclusive formation of organic hydroperoxide products (ROOH) and O_2 is well-established for simple alkyl peroxy radicals such as CH_3O_2 and $C_2H_5O_2$,[5−10] a number of more recent studies have demonstrated that selected oxygenated RO_2 radicals possess significant radical-propagating channels for their reactions with HO_2, thereby lessening their perceived impact as chain terminating processes:[8,11−13]

$$RO_2 + HO_2 \rightarrow RO + OH + O_2 \qquad (1)$$

This may therefore be a contributory factor in systematic under-simulation of HOx radical concentrations observed in the troposphere, as reported in a number of studies.[14−16]

Laboratory studies have shown that channel 1 is particularly significant for the reaction of the acetyl peroxy radical ($CH_3C(O)O_2$) with HO_2, accounting for about 40−50% of the overall reaction,[8,11,13] with more minor contributions in the region of 15−20% also being reported for the reactions of HO_2 with $HOCH_2O_2$,[11] $CH_3C(O)CH_2O_2$,[12,13] and $C_6H_5C(O)O_2$;[13] and for the reaction of HO_2 with the suite of three isomeric RO_2 radicals formed from the reaction of Cl with $C_2H_5C(O)CH_3$.[13] Of these studies, the most direct evidence has been reported by Dillon and Crowley,[13] who measured the formation of OH from the reactions of HO_2 with a number of oxygenated RO_2 radicals directly using pulsed laser photolysis with laser-induced fluorescence detection of OH. They were also able to establish that the radical-propagating channel was insignificant for a number of other oxygenated RO_2 radicals, including several β-hydroxy peroxy radicals formed significantly in the atmosphere from the reactions of OH with alkenes and alcohols.

The studies to date have therefore established the existence of radical-propagating channels for the reactions of HO_2 with oxygenated peroxy radicals containing acyl, α-carbonyl, and α-hydroxy functionalities. However, the importance of such channels has not been considered for peroxy radicals containing an alkoxy group adjacent to the peroxy radical center. The simplest α-alkoxy alkyl peroxy radical (which are derived from the oxidation of ethers in general) is the methoxymethyl peroxy radical ($CH_3OCH_3O_2$). It is formed in the atmosphere from the OH radical initiated oxidation of dimethyl ether, and is also predicted to be generated from the breakdown of a number of complex oxygenated solvents, in particular glycol ethers such as 2-methoxyethanol and 1-methoxypropan-2-ol.[17,18]

The products of the reaction of $CH_3OCH_2O_2$ with HO_2 at 295 K and 700 Torr have previously been studied by the present authors (Wallington et al.[19]), using long path FTIR spectroscopy. Methoxymethyl hydroperoxide (CH_3OCH_2OOH) and methyl formate (CH_3OCHO) were observed as major primary products, the formation of which was attributed to the following radical-terminating reaction channels:

$$CH_3OCH_2O_2 + HO_2 \rightarrow CH_3OCH_2OOH + O_2 \qquad (2a)$$

$$\rightarrow CH_3OCHO + H_2O + O_2 \qquad (2b)$$

Within experimental uncertainties, the yields of CH_3OCH_2OOH and CH_3OCHO provided closure and were used to assign

* Author to whom correspondence should be addressed. E-mail: atmos.chem@btinternet.com.
† Atmospheric Chemistry Services.
‡ Ford Motor Company.

10.1021/jp908158w
Published on Web 11/04/2009

branching ratios of $k_{2a}/k_2 = 0.53 \pm 0.08$ and $k_{2b}/k_2 = 0.40 \pm 0.04$. However, formation of CH_3OCHO could also result from a contribution from a radical-propagating channel (2c),

$$CH_3OCH_2O_2 + HO_2 \rightarrow CH_3OCH_2O + OH + O_2 \quad (2c)$$

followed by the established fates of reaction with O_2 or thermal decomposition for CH_3OCH_2O:[20]

$$CH_3OCH_2O + O_2 \rightarrow CH_3OCHO + HO_2 \quad (3)$$

$$CH_3OCH_2O\ (+M) \rightarrow CH_3OCHO + H\ (+M) \quad (4)$$

$$H + O_2\ (+M) \rightarrow HO_2\ (+M) \quad (5)$$

Based on the reported yield of CH_3OCHO,[19] channel 2c could therefore potentially account for up to about 40% of the reaction.

In the present study, the products of reaction 2 have been reinvestigated at 296 K and 700 Torr using long path FTIR spectroscopy, during photolysis of $Cl_2/CH_3OCH_3/CH_3OH$/air mixtures, the same chemical system employed previously.[19] Similarly to our recent investigations of the reactions of $CH_3C(O)O_2$, $HOCH_2O_2$, and $CH_3C(O)CH_2O_2$ with HO_2,[11,12] the formation of OH radicals in the system has been investigated by addition of benzene to scavenge variable proportions of OH, with the subsequent formation of phenol used as a marker for OH radical formation. Although this method provides an indirect measurement of OH formation, it is noted that our yields reported for the reactions of $CH_3C(O)O_2$ and $CH_3C(O)CH_2O_2$ with HO_2[11,12] are in good agreement with those derived from the direct OH measurements of Dillon and Crowley.[13]

2. Experimental Section

All experiments were performed in the Ford 140 L Pyrex chamber, interfaced with a Mattson Sirius 100 FTIR spectrometer, which is described in detail elsewhere.[21] The chamber is equipped with 22 fluorescent blacklamps (GE F40BLB), emitting near UV radiation in the range 300−450 nm. Radical generation was initiated by the photolysis of Cl_2, with $CH_3OCH_2O_2$ and HO_2 radicals formed from the subsequent reaction of Cl atoms with CH_3OCH_3 and CH_3OH, respectively, by the following well-established mechanisms:

$$Cl_2 + h\nu \rightarrow Cl + Cl \quad (6)$$

$$Cl + CH_3OCH_3 \rightarrow CH_3OCH_2 + HCl \quad (7)$$

$$CH_3OCH_2 + O_2\ (+M) \rightarrow CH_3OCH_2O_2\ (+M) \quad (8a)$$

$$Cl + CH_3OH \rightarrow CH_2OH + HCl \quad (9)$$

$$CH_2OH + O_2 \rightarrow HCHO + HO_2 \quad (10)$$

Benzene was added to the reaction mixtures to scavenge variable proportions of OH radicals generated in the system. Benzene was selected because, unlike CH_3OCH_3 and CH_3OH, it reacts slowly with Cl ($k = 1.3 \times 10^{-16}$ cm^3 molecule^{-1} s^{-1} [22]), but comparatively rapidly with OH ($k_{11} = 1.2 \times 10^{-12}$ cm^3 molecule^{-1} s^{-1} [23]). The formation of phenol from the OH-initiated oxidation of benzene (reactions 11 and 12) was used as the primary diagnostic for OH radical formation, the reported yield of phenol being 53.1 ± 6.6%:[24]

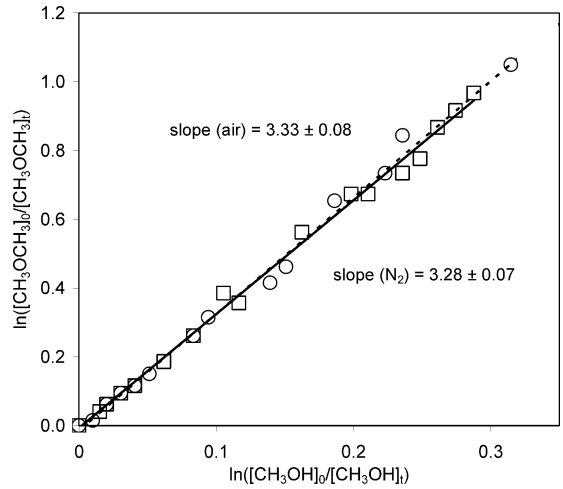

Figure 1. Loss of CH_3OCH_3 versus CH_3OH following exposure to Cl atoms in 700 Torr of N_2 (squares) and air (circles). $[CH_3OH]_0$ and $[CH_3OCH_3]_0$ are the initial concentrations; $[CH_3OH]_t$ and $[CH_3OCH_3]_t$ are concentrations at time = t. $[CH_3OH]_0 \approx 300$ mTorr, $[CH_3OCH_3]_0 \approx 20$ mTorr, and $[Cl_2]_0 \approx 100$ mTorr. Each data set includes combined data from two experiments with the same conditions.

$$OH + C_6H_6\ (+M) \rightarrow HOC_6H_6\ (+M) \quad (11)$$

$$HOC_6H_6 + O_2 \rightarrow C_6H_5OH + HO_2 \quad (12)$$

Infrared spectra of reagents and products were derived from 32 coadded interferograms with a spectral resolution of 0.25 cm^{-1}, and an analytical path length of 27.1 m. All experiments were carried out at 296 (±2) K and 700 Torr total pressure of air.

The organic reagents, CH_3OCH_3 (≥99.9%), CH_3OH (≥99.8%), and benzene (≥99.9%) were obtained from Aldrich Chemical Co. Cl_2 and air were obtained from Michigan Airgas at research grade purity. Reference spectra were obtained by expanding calibrated volumes into the chamber. Unless otherwise specified, all quoted errors are two standard deviations.

3. Results and Discussion

3.1. Rate Coefficient for the Reaction of Cl Atoms with CH_3OCH_3. The relative formation rates of $CH_3OCH_2O_2$ and HO_2 in the experiments described below is determined by the relative rates of reactions 7 and 9. Whereas the value of k_9 is very well determined at temperatures close to 298 K ($k_9 = 5.5 \times 10^{-11}$ cm^3 molecule^{-1} s^{-1}),[23] the six determinations of k_7 show some scatter, covering a range from 1.3×10^{-10} to 2.05×10^{-10} cm^3 molecule^{-1} s^{-1} (see Notario et al.[25] and references therein). Initial experiments were therefore performed in which the loss of CH_3OCH_3 was measured relative to that of CH_3OH during UV irradiation of $Cl_2/CH_3OCH_3/CH_3OH/N_2$ mixtures at 700 Torr (see Figure 1). Linear regression analysis of the data gives a value of $k_7/k_9 = 3.28 \pm 0.07$, this being the key parameter which quantifies the relative formation of $CH_3OCH_2O_2$ and HO_2 in the experiments below. Using the IUPAC recommended value of k_9 given above leads to an absolute value of $k_7 = (1.80 \pm 0.22) \times 10^{-10}$ cm^3 molecule^{-1} s^{-1}, where the quoted error limits

include an additional 10% to account for uncertainty associated with the reference rate coefficient.

The relative loss of CH_3OCH_3 and CH_3OH was also determined during UV irradiation of $Cl_2/CH_3OCH_3/CH_3OH$/air mixtures at 700 Torr, as also shown in Figure 1. The measured relative loss, 3.33 ± 0.08, is indistinguishable from that determined in N_2 diluent, indicating that any secondary chemistry leading to removal of the reagents when O_2 is present (i.e., the formation of OH radicals as described below) does not distort their relative loss significantly. This is as expected, because the relative rate coefficient for the reactions of CH_3OCH_3 and CH_3OH with OH radicals, is very similar in magnitude to the relative rate coefficient for the Cl atom reactions determined above, based on the IUPAC recommended values of $k_{13} = 2.8 \times 10^{-12}$ cm^3 molecule^{-1} s^{-1} and $k_{14} = 9.0 \times 10^{-13}$ cm^3 molecule^{-1} s^{-1}.[23]

$$OH + CH_3OCH_3 \rightarrow CH_2OCH_2 + H_2O \quad (13)$$

$$OH + CH_3OH \rightarrow CH_2OH + H_2O \quad (14a)$$

$$\rightarrow CH_3O + H_2O \quad (14b)$$

For completeness, the relative loss of CH_3OCH_3 and CH_3OH was also analyzed for the set of $Cl_2/CH_3OCH_3/CH_3OH$/benzene/air mixtures used for the analysis described in section 3.3 below. No systematic dependence of the relative loss coefficient was apparent for variation of the initial reagent concentration ratio $[CH_3OH]_0/[CH_3OCH_3]_0$ over the range 2−15, or with the benzene concentration varied over the range from zero up to about 1 Torr (corresponding to up to about 90% scavenging of OH radicals).

3.2. Rate Coefficient for the Reaction of Cl Atoms with Phenol. Phenol is known to react rapidly with Cl atoms to produce phenoxy radicals (reaction 15), and it is important to quantify the associated removal of phenol under the experimental conditions employed. In our previous studies,[11] an apparent lowering of k_{15} was observed in experiments performed in the presence of O_2, and this was tentatively attributed to the partial regeneration of phenol from the reaction of phenoxy radicals with species containing labile hydrogen atoms, for example HO_2 (reaction 16):

$$Cl + C_6H_5OH \rightarrow HCl + C_6H_5O \quad (15)$$

$$C_6H_5O + HO_2 \rightarrow C_6H_5OH + O_2 \quad (16)$$

To characterize this for the current system, a series of experiments was performed in which the loss of phenol was measured relative to that of CH_3OCH_3 during UV irradiation of Cl_2/phenol/CH_3OCH_3 and Cl_2/phenol/CH_3OCH_3/CH_3OH mixtures (see Figure 2). The employed initial concentrations of Cl_2, CH_3OCH_3, and CH_3OH were typical of those in the experiments described below (section 3.3), and the initial concentration of phenol was comparable with the final concentrations generated in the those experiments when about 1 Torr of benzene was present. The experiments were performed in 700 Torr of either N_2 or air.

Figure 2 shows a plot of the decay of phenol versus CH_3OCH_3 observed in the photolysis experiments (N.B., corrections of up to about 20% have been applied to the phenol data to account for its thermal heterogeneous loss in the chamber, as characterized and described previously[11]). The results of the Cl_2/phenol/CH_3OCH_3 experiment in N_2 diluent provide a measure of the rate constant ratio $k_{15}/k_7 = 1.07 \pm 0.05$. Using the value of k_7 determined above, this leads to an absolute value of $k_{15} = (1.93 \pm 0.25) \times 10^{-10}$ cm^3 molecule^{-1} s^{-1}, in excellent agreement with the values of $k_{15} = (1.92 \pm 0.17) \times 10^{-10}$ cm^3 molecule^{-1} s^{-1} and $k_{15} = (1.93 \pm 0.36) \times 10^{-10}$ cm^3 molecule^{-1} s^{-1} reported previously.[11,26] The results of a corresponding experiment performed in air diluent indicate a lowering of the measured rate coefficient ratio to a value of 0.814 ± 0.018 (see Figure 2), consistent with an apparent rate coefficient $k_{15obs} = (1.47 \pm 0.18) \times 10^{-10}$ cm^3 molecule^{-1} s^{-1}. As indicated above, the apparent decrease in the reactivity of phenol possibly reflects its partial re-formation by reactions with hydrogen containing species (e.g., HO_2 radicals) formed during the oxidation reactions that occur in air diluent. The abundance of HO_2 was therefore increased by addition of CH_3OH to the reaction mixture such that $[CH_3OH]_0/[CH_3OCH_3]_0$ was typical of the high end of the range employed in the experiments reported below. This led to a further lowering of the measured rate coefficient ratio to a value of 0.701 ± 0.024 (see Figure 2), consistent with an apparent rate coefficient $k_{15obs} = (1.26 \pm 0.16) \times 10^{-10}$ cm^3 molecule^{-1} s^{-1}, providing some support for phenol regeneration via reaction 16. These values of k_{15obs}, obtained in air with concentrations of CH_3OCH_3 and CH_3OH characteristic of those used in the subsequent experiments, were therefore used in the studies described below, either to correct the phenol yields for its net loss via reaction 15 or to calculate the reaction rate in simulations.

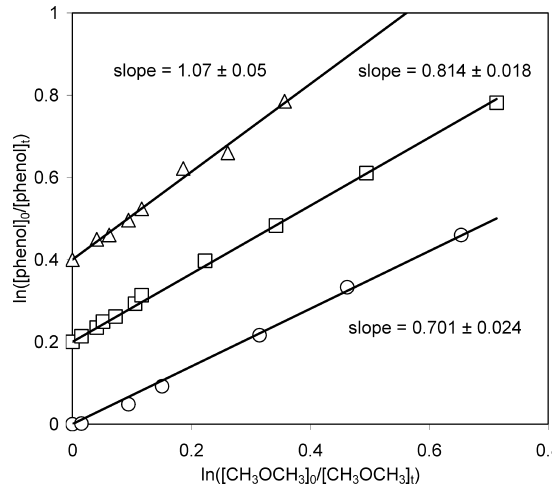

Figure 2. Loss of phenol versus CH_3OCH_3 following exposure to Cl atoms. $[phenol]_0$ and $[CH_3OCH_3]_0$ are the initial concentrations; $[phenol]_t$ and $[CH_3OCH_3]_t$ are concentrations at time = t. Triangles are Cl_2/CH_3OCH_3/phenol experiment in 700 Torr N_2 ($[phenol]_0$ = 2.9 mTorr; $[CH_3OCH_3]_0$ = 20.0 mTorr). Squares are Cl_2/CH_3OCH_3/phenol experiment in 700 Torr air ($[phenol]_0$ = 2.9 mTorr; $[CH_3OCH_3]_0$ = 20.0 mTorr). Circles are $Cl_2/CH_3OCH_3/CH_3OH$/phenol experiment in 700 Torr air ($[phenol]_0$ = 3.1 mTorr; $[CH_3OCH_3]_0$ = 20.6 mTorr; $[CH_3OH]_0$ = 307 mTorr). For clarity, the first two data sets been offset vertically by 0.4 and 0.2, respectively.

3.3. Investigation of the $Cl_2/CH_3OCH_3/CH_3OH$/Benzene/Air System. ***3.3.1. Analysis and Interpretation of Phenol Formation.*** The reaction of $CH_3OCH_2O_2$ with HO_2 (reaction 2) was investigated in a series of $Cl_2/CH_3OCH_3/CH_3OH$/benzene/air UV photolysis experiments in which the ratio of the peroxy radical precursor concentration, $[CH_3OH]_0/[CH_3OCH_3]_0$ was varied from a value of zero up to about 15. This leads to corresponding relative primary production rates

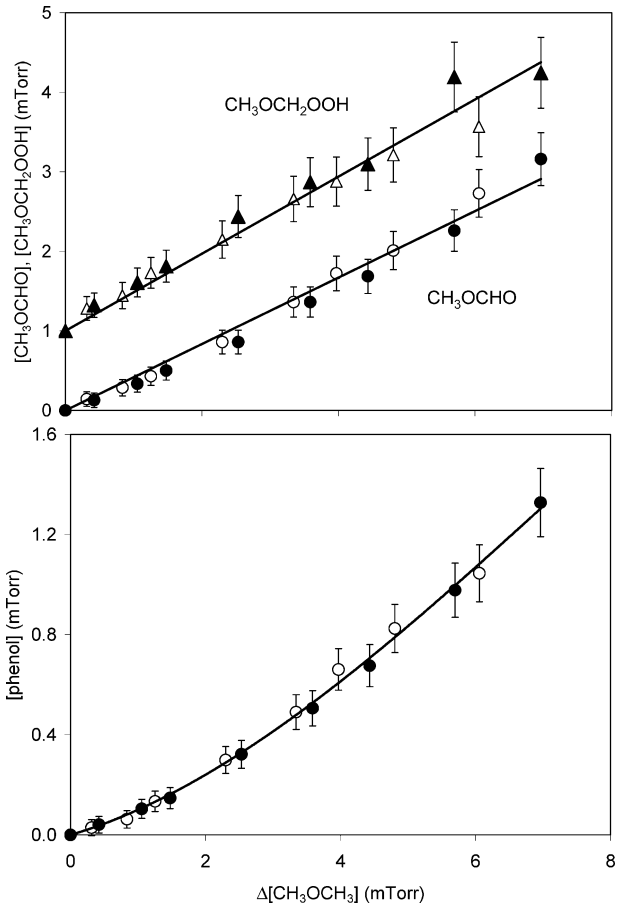

Figure 3. Yields of CH_3OCHO, CH_3OCH_2OOH, and phenol relative to CH_3OCH_3 lost during the photolysis of $Cl_2/CH_3OCH_3/CH_3OH$/benzene/air mixtures. (For clarity CH_3OCH_2OOH data have been offset vertically by 1 mTorr.) Displayed data are from repeat experiments A (closed symbols) and L (open symbols) with $[CH_3OH]_0/[CH_3OCH_3]_0 \approx 15$ and about 1 Torr of benzene present. Product yields have been corrected for losses in the system ($\leq$0.2%, $\leq$8%, and $\leq$20% for CH_3OCHO, CH_3OCH_2OOH, and phenol, respectively). Lines for CH_3OCHO and CH_3OCH_2OOH are linear regressions of the combined data, consistent with respective yields of 0.42 and 0.49 relative to CH_3OCH_3 lost. The line for phenol is a third-order polynomial fit to the combined data: $y = 0.0787x + 0.0228x^2 - 0.0010x^3$, indicative of primary and delayed formation in the system.

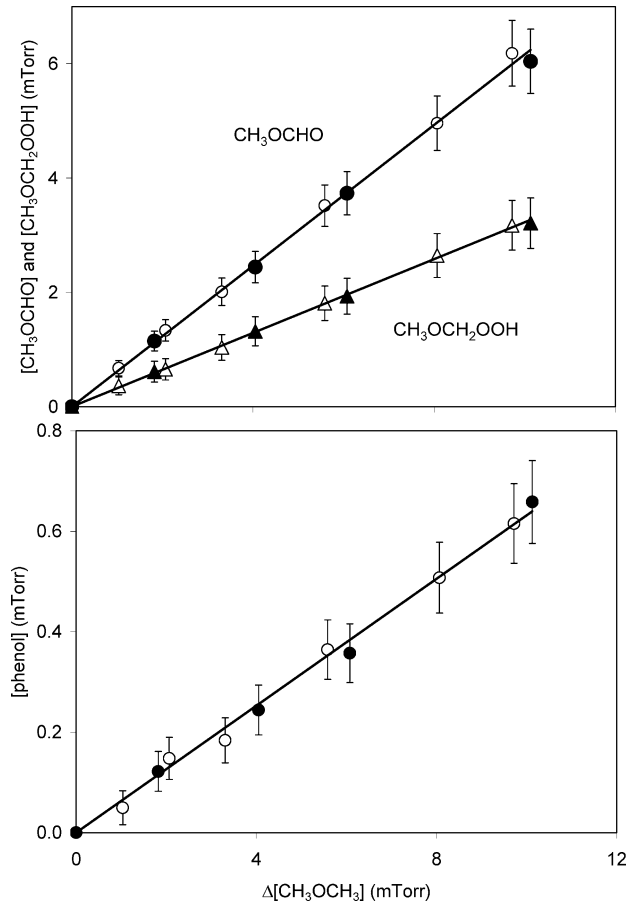

Figure 4. Yields of CH_3OCHO, CH_3OCH_2OOH, and phenol relative to CH_3OCH_3 lost during the photolysis of Cl_2/CH_3OCH_3/benzene/air mixtures. Displayed data are from the repeat experiments C (closed symbols) and M (open symbols) in the absence of CH_3OH and with about 1 Torr of benzene present. Product yields have been corrected for losses in the system ($\leq$0.3%, $\leq$14%, and $\leq$30% for CH_3OCHO, CH_3OCH_2OOH, and phenol, respectively). Lines are linear regressions of the combined data, consistent with respective yields of 0.62, 0.32, and 0.063 relative to CH_3OCH_3 lost for CH_3OCHO, CH_3OCH_2OOH, and phenol.

of HO_2 and $CH_3OCH_2O_2$, which vary over the approximate range 0−5, and an associated variation in the relative steady state concentrations of the peroxy radicals. At the high end of the $[CH_3OH]_0/[CH_3OCH_3]_0$ range, $CH_3OCH_2O_2$ is lost mainly through its reaction with HO_2, with removal via its self-reaction making an increasing contribution toward the low end of the $[CH_3OH]_0/[CH_3OCH_3]_0$ range, as described further below.

As in our previous study,[19] the formation of CH_3OCHO and CH_3OCH_2OOH was observed in experiments over the entire $[CH_3OH]_0/[CH_3OCH_3]_0$ range. The upper panels of Figures 3 and 4 show examples of the formation of these products vs CH_3OCH_3 removed, for respective $[CH_3OH]_0/[CH_3OCH_3]_0$ ratios of about 15 and zero. The plots demonstrate that both CH_3OCHO and CH_3OCH_2OOH are primary products, with the slopes of the plots allowing quantification of the yields. The yields obtained in all the experiments listed in Table 1 are shown in the upper panel of Figure 5, as a function of $[CH_3OH]_0/[CH_3OCH_3]_0$. The magnitudes of these yields, and their dependence on $[CH_3OH]_0/[CH_3OCH_3]_0$, are fully consistent with those reported in our previous study.[19] At the high end of the

TABLE 1: Summary of Experimental Conditions in $Cl_2/CH_3OCH_3/CH_3OH$/Benzene/Air Experiments (Section 3.3)

run	$[Cl_2]_0$ (mTorr)	$[CH_3OCH_3]_0$ (mTorr)	$[CH_3OH]_0$ (mTorr)	$[benzene]_0$ (mTorr)	$[CH_3OH]_0/[CH_3OCH_3]_0$	f_{OH}
A	100	21.1	298	1017	14.1	0.79
B	100	20.9	158	1017	7.6	0.86
C	100	20.3	0	1034	0	0.96
D	101	21.1	44.9	1034	2.1	0.93
E	100	21.1	234	1051	11.1	0.82
F	199	41.8	634	1017	15.2	0.64
G	100	21.1	317	98.3	15.0	0.26
H	102	20.7	312	0	15.1	0
I	103	20.9	317	50.9	15.2	0.15
J	100	20.9	322	225	15.4	0.44
K	101	21.1	317	559	15.0	0.66
L	101	20.9	322	1034	15.4	0.78
M	100	20.7	0	1017	0	0.95

$[CH_3OH]_0/[CH_3OCH_3]_0$ range, yields of 0.42 ± 0.06 and 0.51 ± 0.10 were obtained for CH_3OCHO and CH_3OCH_2OOH, respectively, on the basis of all the experiments with $[CH_3OH]_0/[CH_3OCH_3]_0 \approx 15$, with the error limits including 5% and 10% uncertainties associated with the quantification of the two products.[19] In the absence of CH_3OH (i.e., $[CH_3OH]_0/$

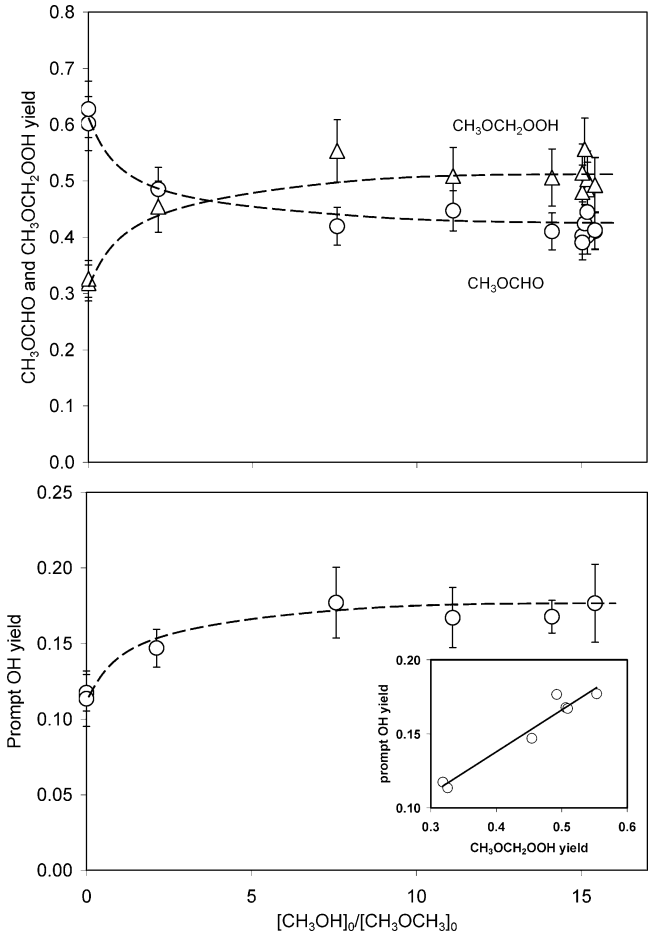

Figure 5. Yields of CH_3OCHO, CH_3OCH_2OOH, and prompt OH, relative to CH_3OCH_3 lost, as a function of $[CH_3OH]_0/[CH_3OCH_3]_0$ during the photolysis of Cl_2/CH_3OCH_3/benzene/air mixtures. Displayed data for CH_3OCHO and CH_3OCH_2OOH are from all experiments in Table 1. The prompt OH yields were derived from the initial formation of phenol in experiments A−E, L, and M with $f_{OH} \geq 0.78$ (see text). The broken lines are arbitrary functions included to aid in visual inspection of the data trends. The lower panel inset shows a correlation of the yields of prompt OH and CH_3OCH_2OOH.

$[CH_3OCH_3]_0 = 0$), the yield of CH_3OCHO increases to 0.62 ± 0.06, and that of CH_3OCH_2OOH decreases to 0.32 ± 0.04, in excellent agreement with those reported in our previous studies.[19,20] In the absence of CH_3OH, there is no primary route to HO_2 formation. However, $CH_3OCH_2O_2$ radicals are initially removed by their self-reaction,

$$CH_3OCH_2O_2 + CH_3OCH_2O_2 \rightarrow CH_3OCH_2O + CH_3OCH_2O + O_2 \quad (17a)$$

$$\rightarrow CH_3OCHO + CH_3OCH_2OH + O_2 \quad (17b)$$

with the subsequent reactions of CH_3OCH_2O (formed with approximately 70% yield via channel 17a) leading to secondary HO_2 formation (via reaction 3 or reactions 4 and 5). As a result, reaction with HO_2 radicals makes a reduced, but still substantial, contribution to $CH_3OCH_2O_2$ removal under steady state photolysis conditions, even when CH_3OH is absent. Consequently, products such as CH_3OCH_2OOH (formed exclusively from the reaction of $CH_3OCH_2O_2$ with HO_2) are still generated significantly in the absence of CH_3OH.

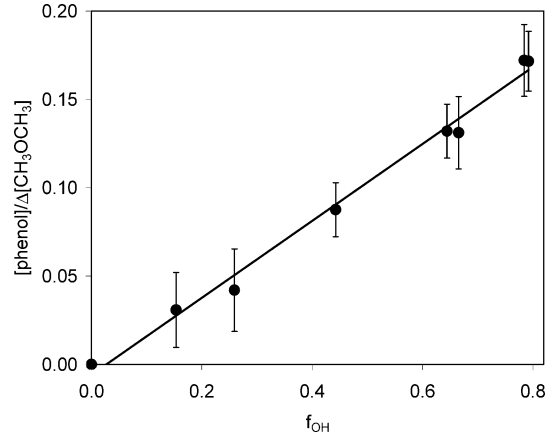

Figure 6. Observed yield of phenol vs the calculated fraction of OH scavenged by reaction with benzene (f_{OH}), in experiments A and F−L with $[CH_3OH]_0/[CH_3OCH_3]_0 \approx 15$ (see Table 1). Determination of f_{OH} based on $k_{11} = 1.2 \times 10^{-12}$ cm^3 molecule^{-1} s^{-1}, $k_{13} = 2.8 \times 10^{-12}$ cm^3 molecule^{-1} s^{-1}, and $k_{14} = 9.0 \times 10^{-13}$ cm^3 molecule^{-1} s^{-1} from the current IUPAC evaluation.[23] Phenol yields determined at 5 mTorr consumption of CH_3OCH_3.

The experiments were carried out with benzene present in the reaction mixtures at pressures up to about 1 Torr. Owing to its extremely low reactivity with Cl, benzene at these pressures does not interfere with the production of $CH_3OCH_2O_2$ and HO_2 under the conditions employed (scavenging $\leq 0.002\%$ of Cl atoms) but is sufficiently reactive to scavenge OH radicals in competition with other reactions of OH (i.e., primarily its reactions with CH_3OCH_3 and CH_3OH, reactions 13 and 14), leading to the formation of phenol by reaction sequences 11 and 12. Accordingly, phenol formation was observed in all experiments in which benzene was added (over the entire $[CH_3OH]_0/[CH_3OCH_3]_0$ range), with the structured infrared band near 750 cm^{-1} allowing its sensitive and specific detection and quantification.[11]

The lower panels of Figures 3 and 4 show the formation of phenol vs CH_3OCH_3 removed, in the example experiments discussed above, with $[CH_3OH]_0/[CH_3OCH_3]_0$ ratios of about 15 and 0. In these experiments, approximately 1 Torr of benzene was present, allowing between 78% and 96% of OH to be scavenged by reaction 11. At high $[CH_3OH]_0/[CH_3OCH_3]_0$ (Figure 3), the curved plot demonstrates that phenol is generated as a primary product, indicative of prompt formation of OH, but with this formation supplemented by one or more additional sources of OH at greater extents of reaction. In the absence of CH_3OH (Figure 4), however, the linearity of the plot suggests that phenol is formed almost exclusively as a prompt primary product, suggesting that secondary sources of OH are much less important under these conditions. These observations are consistent with the majority of the delayed OH production being due to the chemistry initiated by the reaction of HO_2 with the major product HCHO (formed from CH_3OH oxidation, primarily by reaction sequences 9 and 10) to form $HOCH_2O_2$, which has been fully characterized and described previously.[11] OH formation associated with this chemistry was found to result from the radical propagating channel for the reaction of $HOCH_2O_2$ with HO_2, and also from the reaction of Cl atoms with the terminating channel product, $HOCH_2OOH$.

The initial yields of phenol (denoted $[phenol]_{initial}$), derived either from the linear component of the polynomial fits or from

TABLE 2: Supplementary Reaction Mechanism and Associated Parameters Used To Simulate the Cl/CH_3OCH_3/CH_3OH/Benzene/Air Photolysis Experiments[a]

			branching ratio	rate coefficient[c]	comment
		Initiation Reactions			
$Cl + CH_3OCH_3$ $(+O_2)$	$\rightarrow CH_3OCH_2O_2 + HCl$	(7) + (8a)	0.986	1.8×10^{-10}	*d, e*
	$\rightarrow HCHO + HCHO + OH + HCl$	(7) + (8b)	0.014		
$OH + CH_3OCH_3$ $(+O_2)$	$\rightarrow CH_3OCH_2O_2 + H_2O$	(13) + (8a)	0.986	$5.7 \times 10^{-12} \exp(-215/T)$	*f, e*
	$\rightarrow HCHO + HCHO + OH + H_2O$	(13) + (8b)	0.014		
		$RO_2 + HO_2$ Reactions			
$CH_3OCH_2O_2 + HO_2$	$\rightarrow CH_3OCH_2OOH + O_2$	(2a)	varied (see text)	1.0×10^{-11}	*g*
	$\rightarrow CH_3OCHO + H_2O + O_2$	(2b)			
	$\rightarrow CH_3OCH_2O + OH + O_2$	(2c)			
		$RO_2 + RO_2$ Reactions			
$2\ CH_3OCH_2O_2$	$\rightarrow 2\ CH_3OCH_2O + O_2$	(17a)	0.67	2.1×10^{-12}	*h*
	$\rightarrow CH_3OCHO + CH_3OCH_2OH + O_2$	(17b)	0.33		
$CH_3OCH_2O_2 + HOCH_2O_2$	$\rightarrow CH_3OCH_2O + HOCH_2O + O_2$		0.774	3.46×10^{-12}	*i*
	$\rightarrow CH_3OCHO + HOCH_2OH + O_2$		0.113		
	$\rightarrow CH_3OCH_2OH + HCOOH + O_2$		0.113		
$CH_3OCH_2O_2 + \Phi{-}O_2$	$\rightarrow CH_3OCH_2O + \Phi{-}O + O_2$		0.5	2.0×10^{-12}	*j*
	$\rightarrow CH_3OCHO + \Phi{-}OH + O_2$		0.5		
		RO Reactions			
$CH_3OCH_2O + O_2$	$\rightarrow CH_3OCHO + HO_2$	(3)		assumed instantaneous	*k*
		Cl + Product Reactions			
$Cl + CH_3OCHO$	$\rightarrow$ products			1.3×10^{-12}	*l, m*
$Cl + CH_3OCH_2OH$ $(+O_2)$	$\rightarrow CH_3OCHO + HO_2 + HCl$			5.0×10^{-11}	*n*
$Cl + CH_3OCH_2OOH$	$\rightarrow CH_3OCHO + OH + HCl$	(18) + (19)		6.1×10^{-11}	*o*
		OH + Product Reactions			
$OH + CH_3OCHO$	$\rightarrow$ products			$9.39 \times 10^{-13} \exp(-461/T)$	*p, m*
$OH + CH_3OCH_2OH$ $(+O_2)$	$\rightarrow CH_3OCHO + HO_2 + H_2O$			4.56×10^{-12}	*q*
$OH + CH_3OCH_2OOH$	$\rightarrow CH_3OCH_2O_2 + H_2O$		0.286	1.26×10^{-11}	*q*
	$\rightarrow CH_3OCHO + OH + H_2O$		0.714		

[a] These reactions were used in conjunction with relevant chemistry in Table 3 of Jenkin et al.[11] (see note *b*). The reaction number in the text is shown in brackets where applicable. [b] The Cl/CH_3OH/benzene/air system was previously characterized within study of the reaction of $CH_3C(O)O_2$ with HO_2.[11] Relevant reactions were used in the present simulations, with the adjustments to k_{15obs} described in section 3.2. [c] Units cm^3 $molecule^{-1}$ s^{-1}. [d] Rate coefficient (k_7) determined in the present study, relative to a value of 5.5×10^{-11} cm^3 $molecule^{-1}$ s^{-1} for k_9. [e] Branching ratio for the consecutive reaction of $CH_3OCH_2 + O_2$, based on Sehested et al.[27] [f] Rate coefficient based on current IUPAC recommendation.[23] [g] Rate coefficient estimated by Jenkin et al.;[20] branching ratios were varied on the basis of the results of the present study and Wallington et al.[19] [h] Rate coefficient and branching ratios from Jenkin et al.[20] [i] Rate coefficient based on geometric mean of self-reaction rate coefficients for $CH_3OCH_2O_2$ and $HOCH_2O_2$; branching ratios based on arithmetic mean of branching ratios for self-reactions of $CH_3OCH_2O_2$ and $HOCH_2O_2$. [j] Rate coefficients and branching ratios estimated on the basis of known reactions of peroxy radicals. "Φ-O_2" represents the complex organic peroxy radical, formed from OH + benzene (see Jenkin et al.[11]). [k] RO reactions occur on ≤ 30 μs time scale. Reaction with O_2 estimated to dominate over decomposition by H atom ejection, based on Jenkin et al.,[20] although ultimate products under experimental conditions are indistinguishable. [l] Rate coefficient from Wallington et al.[28] [m] Products not declared, because $\leq 0.3\%$ removal of CH_3OCHO occurred under experimental conditions. [n] Kinetic parameters estimated on the basis of known reactivity of Cl with species containing $-OH$ groups. [o] Rate coefficient from Wallington et al.;[19] products defined by analogy with chemistry of CH_3OOH and CH_2OOH, Vaghjiani and Ravishankara.[29] [p] Rate coefficient based on Wallington et al.[30] and Le Calvé et al.,[31] as described by Jenkin and Hayman.[32] [q] Kinetic parameters estimated on the basis of known reactivity of OH with oxygen-bridged species and species containing $-OH$ and $-OOH$ groups.

a linear regression of the data where appropriate, were used to determine the prompt yield of OH, as follows:

$$\text{prompt OH yield} = ([\text{phenol}]_{\text{initial}}/\Delta[CH_3OCH_3])/(0.531 f_{OH}) \quad \text{(i)}$$

$$f_{OH} = k_{11}[\text{benzene}]_0/(k_{11}[\text{benzene}]_0 + k_{13}[CH_3OCH_3]_0 + k_{14}[CH_3OH]_0) \quad \text{(ii)}$$

Here, f_{OH} is the calculated fraction of OH which reacts with benzene (reaction 11) under the experimental conditions, and the factor 0.531 in equation (i) is the yield of phenol from this reaction (i.e., via reaction sequence 11 and 12). The resultant OH yields are plotted in the lower panel of Figure 5, as a function of $[CH_3OH]_0/[CH_3OCH_3]_0$, for all experiments with values of $f_{OH} \geq 0.78$. Toward the high end of the $[CH_3OH]_0/[CH_3OCH_3]_0$ range, a limiting OH yield of about 0.18 was determined, with the yield falling to about 0.11 in the absence of CH_3OH (i.e., $[CH_3OH]_0/[CH_3OCH_3]_0 = 0$). The relative dependence of the prompt OH yield on $[CH_3OH]_0/[CH_3OCH_3]_0$ is strikingly similar to that observed for CH_3OCH_2OOH, as confirmed by the correlation in Figure 5 (lower panel inset). This provides strong support for the prompt OH formation resulting mainly from the reaction of $CH_3OCH_2O_2$ with HO_2, via channel 2c. The OH yield at high $[CH_3OH]_0/[CH_3OCH_3]_0$ (i.e., when $CH_3OCH_2O_2$ reacts mainly with HO_2) thus provides an initial estimate of the branching ratio $k_{2c}/k_2 \approx 0.18$.

As in our previous studies,[11,12] a series of experiments with a high precursor concentration ratio ($[CH_3OH]_0/[CH_3OCH_3]_0 \approx 15$) was also carried out with a series of benzene concentrations over the range from zero up to about 1 Torr (see Table 1). This was to confirm that phenol formation was due to the OH-initiated oxidation of benzene, and not via some alternative oxidation mechanism not requiring OH formation. The resultant

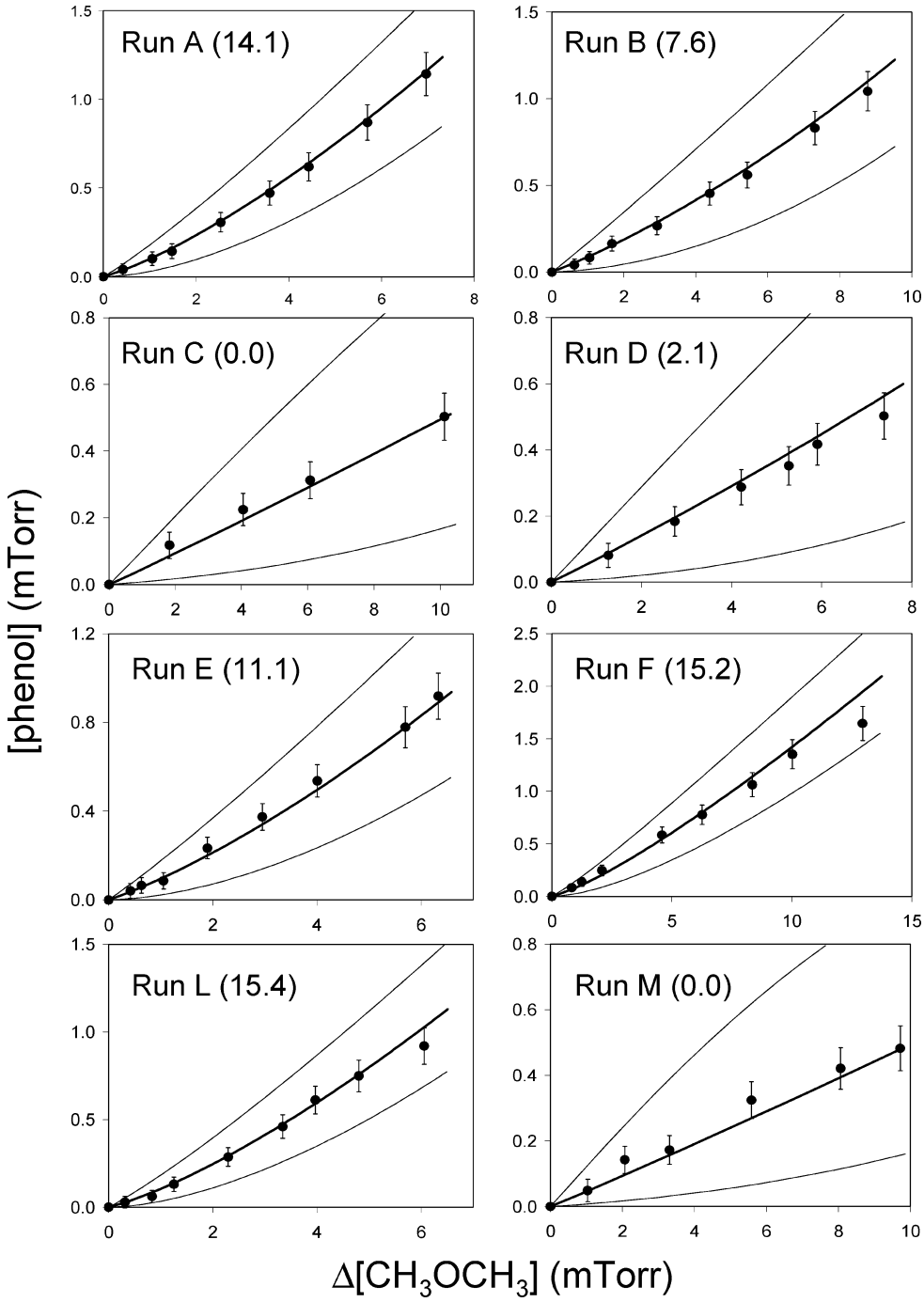

Figure 7. Formation of phenol vs CH_3OCH_3 removed in all experiments with approximately 1 Torr of benzene present. The figures in brackets are the ratio $[CH_3OH]_0/[CH_3OCH_3]_0$ (see Table 1). The points are the observed concentrations. The lines are simulations using the mechanism in Table 2. The bold lines are simulations with the optimized value of $k_{2c}/k_2 = 0.19$. The upper and lower lines are simulations with $k_{2c}/k_2 = 0.4$ and $k_{2c}/k_2 = 0.0$, respectively (corrections of up to 5% have been applied to the observed phenol concentration data to correct for its thermal heterogeneous loss, as described in section 3.2).

phenol yields are presented in Figure 6 as a function of f_{OH}. Because quantification of the initial slope, $[\text{phenol}]_{\text{initial}}/\Delta[CH_3OCH_3]$, was unreliable in experiments with lower benzene concentrations present, the phenol yields were based on total phenol formation at 5 mTorr consumption of CH_3OCH_3 in each experiment The results in Figure 6 confirm a linear dependence of phenol formation on f_{OH}, consistent with its production being due to the reaction of OH with benzene occurring in competition with reactions 13 and 14a.

3.3.2. Numerical Simulation of the System. The system was also characterized by simulation using a detailed explicit mechanism, which is shown partially in Table 2. The reactions listed in the table were used to supplement a detailed mechanism which was optimized previously for the Cl/CH_3OH/benzene/air system, as a component part of our study of the reaction of $CH_3C(O)O_2$ with HO_2.[11] The supplementary chemistry shown in Table 2 thus treats the initial stages of CH_3OCH_3 degradation, including its reactions with Cl and OH, the reactions of $CH_3OCH_2O_2$ with the suite of peroxy radicals formed in the system (i.e., HO_2, $CH_3OCH_2O_2$, $HOCH_2O_2$, and Φ-O_2), and the further reactions of products specific to this system (e.g., CH_3OCH_2OOH).

Simulations of all the experiments indicated that they were well described using a value of $k_{2c}/k_2 = 0.19 \pm 0.03$, with these uncertainty limits representing statistical errors alone. This was based on a global fit to the experiments illustrated in Figure 7, which are those in which high benzene concentrations (≈1 Torr) were used. The results clearly indicate that the observed phenol formation, particularly at low reagent conversions, cannot be accounted for without the participation of the radical-propagating channel, reaction 2c. The consistent performance of the mechanism across the complete range of $[CH_3OH]_0/[CH_3OCH_3]_0$ also confirms that the competition between reactions 2 and 17 for $CH_3OCH_2O_2$ is adequately described by the parameters applied. This provides support for the relative production rates simulated for $CH_3OCH_2O_2$ and HO_2, and for the rate coefficients applied to reactions 2 and 17. Whereas k_{17} was measured directly in our previous study,[20] the applied value of k_2 (1×10^{-11} cm^3 molecule^{-1} s^{-1}) is based on that inferred previously from the relative steady state concentrations of $CH_3OCH_2O_2$ and HO_2 observed in molecular modulation experiments.[20] On the basis of this analysis, we report a value of $k_{2c}/k_2 = 0.19 \pm 0.08$, where the error limits include a 25% contribution from possible systematic errors in the above analysis. This figure is based on an appraisal of the sensitivity of the system to varying the key rate coefficients in Table 2 over realistic uncertainty ranges, and includes uncertainties associated with the yield of phenol from the OH-initiated oxidation of benzene.

Figure 7 also shows the results of simulations in which k_{2c}/k_2 was set to values of 0.4 and zero. The latter case demonstrates the contribution from other sources of OH in the system. These are most notable at high $[CH_3OH]_0/[CH_3OCH_3]_0$, where substantial secondary OH production results from the chemistry of $HOCH_2O_2$ formed from the reaction of HO_2 with HCHO, as indicated above and characterized previously.[11] In the absence of CH_3OH (i.e., $[CH_3OH]_0/[CH_3OCH_3]_0 = 0$), significant formation of HCHO does not occur and the observed formation of phenol is dominated throughout by the production of OH via reaction 2c, which is simulated to account for 73% of the integrated OH produced for a CH_3OCH_3 depletion of 5 mTorr (i.e., about 20% depletion). The residual production of OH under these conditions is partially accounted for by the secondary removal of CH_3OCH_2OOH, as follows,

$$Cl + CH_3OCH_2OOH \rightarrow CH_3OCHOOH + HCl \quad (18)$$

$$CH_3OCHOOH \rightarrow CH_3OCHO + OH \quad (19)$$

which is simulated to account for about 15% of the integrated OH produced. The remaining 12% is due to direct formation from the minor channel of the reaction of CH_3OCH_2 with O_2:

$$CH_3OCH_2 + O_2 \rightarrow HCHO + HCHO + OH \quad (8b)$$

This accounts for 1.4% of this reaction at 700 Torr, based on the parameters derived by Sehested et al.[27] Support for this level of contribution was provided by the observed formation of trace amounts of HCHO, which agreed well with those simulated.

For the above analysis, the balance of reaction 2 was divided between channels 2a and 2b, with branching ratios $k_{2a}/k_2 = 0.6$ and $k_{2b}/k_2 = (0.4 - k_{2c}/k_2)$. These ratios correspond to respective yields of CH_3OCH_2OOH and CH_3OCHO of 0.6 and 0.4 from reaction 2, which are broadly consistent with those reported above, and previously,[19] for experiments at high $[CH_3OH]_0/[CH_3OCH_3]_0$. The formation of CH_3OCH_2OOH and CH_3OCHO actually observed in the present experiments with $[CH_3OH]_0/[CH_3OCH_3]_0 \approx 15$ was also used to provide optimized values of k_{2a}/k_2 and $(k_{2b} + k_{2c})/k_2$. For this procedure, k_{2c}/k_2 was fixed at a value of 0.19 on the basis of the results of the phenol analysis above, and compensating changes were made to the branching ratio not being optimized (i.e., k_{2b}/k_2 when optimizing k_{2a}/k_2, and vice versa) to account for the balance of the reaction. This provided optimized values of $k_{2a}/k_2 = 0.55 \pm 0.05$ and $(k_{2b} + k_{2c})/k_2 = 0.39 \pm 0.04$. This analysis also confirmed that the modest variations applied to k_{2a}/k_2 and k_{2b}/k_2 during this procedure had a negligible impact on simulated formation of phenol. After inclusion of 5% and 10% uncertainties associated with the quantification of CH_3OCHO and CH_3OCH_2OOH,[19] this leads to values of $k_{2a}/k_2 = 0.55 \pm 0.08$ and $(k_{2b} + k_{2c})/k_2 = 0.39 \pm 0.05$. These branching ratios are therefore consistent with channels 2a−2c accounting for the entire reaction, within experimental uncertainties.

4. Conclusions and Atmospheric Implications

The results presented above provide further evidence that the reactions of HO_2 with selected oxygenated RO_2 radicals proceed partially via radical-propagating channels, thereby lessening their perceived impact as chain terminating processes in the atmosphere. The existence of such channels has previously been reported for the reactions of HO_2 with examples of acyl ($CH_3C(O)O_2$[8,11,13] and $C_6H_5C(O)O_2$[13]), α-carbonyl ($CH_3C(O)CH_2O_2$[12,13] and RO_2 radicals produced from $C_2H_5C(O)CH_3$[13]), and α-hydroxy ($HOCH_2O_2$[11]) peroxy radicals. The present work adds the simplest α-alkoxy peroxy radical, $CH_3OCH_2O_2$, to this list. It therefore appears that a channel producing OH radicals exists for the reactions of HO_2 with peroxy radicals containing a number of oxygenated substitutions of atmospheric significance. As indicated in section 1, it has been recognized recently that such reactions probably make a contribution to the unexpectedly high HO_x concentrations observed in locations where reaction with HO_2 radicals is believed to be an important fate of organic peroxy radicals.[14−16] A precise estimation of this contribution awaits a more detailed understanding of the factors which influence organic oxidation chemistry under low NO_x conditions. Further experimental and theoretical work in this area is needed.

References and Notes

(1) Wallington, T. J.; Dagaut, P.; Kurylo, M. J. *Chem. Rev.* **1992**, *92*, 667.

(2) Lightfoot, P. D.; Cox, R. A.; Crowley, J. N.; Destriau, M.; Hayman, G. D.; Jenkin, M. E.; Moortgat, G. K.; Zabel, F. *Atmos. Environ.* **1992**, *26A*, 1805.

(3) Tyndall, G. S.; Cox, R. A.; Granier, C.; Lesclaux, R.; Moortgat, G. K.; Pilling, M. J.; Ravishankara, A. R.; Wallington, T. J. *J. Geophys. Res. D* **2001**, *106*, 12157.

(4) Jenkin, M. E.; Clemitshaw, K. C. *Atmos. Environ.* **2000**, *34*, 2499.

(5) Wallington, T. J. *J. Chem. Soc., Faraday Trans.* **1991**, *87*, 2379.

(6) Spittler, M.; Barnes, I.; Becker, K. H.; Wallington, T. J. *Chem. Phys. Lett.* **2000**, *321*, 57.

(7) Elrod, M. J.; Ranschaert, D. L.; Schneider, N. J. *Int. J. Chem. Kinet.* **2001**, *33*, 363.

(8) Hasson, A. S.; Tyndall, G. S.; Orlando, J. J. *J. Phys. Chem. A* **2004**, *108*, 5979.

(9) Raventós-Duran, M. T.; Percival, C. J.; McGillen, M. R.; Hamer, P. D.; Shallcross, D. E. *Phys. Chem. Chem. Phys.* **2007**, *9*, 4338.

(10) Raventós-Duran, M. T.; McGillen, M. R.; Percival, C. J.; Hamer, P. D.; Shallcross, D. E. *Int. J. Chem. Kinet.* **2007**, *39*, 571.

(11) Jenkin, M. E.; Hurley, M. D.; Wallington, T. J. *Phys. Chem. Chem. Phys.* **2007**, *9*, 3149.

(12) Jenkin, M. E.; Hurley, M. D.; Wallington, T. J. *Phys. Chem. Chem. Phys.* **2008**, *10*, 4274.

(13) Dillon, T. J.; Crowley, J. N. *Atmos. Chem. Phys.* **2008**, *8*, 4877.

(14) Thornton, J. A.; Wooldridge, P. J.; Cohen, R. C.; Martinez, M.; Harder, H.; Brune, W. H.; Williams, E. J.; Roberts, J. M.; Fehsenfeld, F. C.; Hall, S. R.; Shetter, R. E.; Wert, B. P.; Fried, A. *J. Geophys. Res.* **2002**, *107* (D12), 4146 (doi: 10.1029/2001JD000932).

(15) Butler, T. M.; Taraborrelli, D.; Brühl, C.; Fischer, H.; Harder, H.; Martinez, M.; Williams, J.; Lawrence, M. G.; Lelieveld, J. *Atmos. Chem. Phys.* **2008**, *8*, 4529.

(16) Hofzumahaus, A.; Rohrer, F.; Lu, K. D.; Bohn, B.; Brauers, T.; Chang, C. C.; Fuchs, H.; Holland, F.; Kita, K.; Kondo, Y.; Li, X.; Lou, S. R.; Shao, M.; Zeng, L. M.; Wahner, A.; Zhang, Y. H. *Science* **2009**, *324*, 1702.

(17) Jenkin, M. E.; Saunders, S. M.; Pilling, M. J. *Atmos. Environ.* **1997**, *31*, 81.

(18) Saunders, S. M.; Jenkin, M. E.; Derwent, R. G.; Pilling, M. J. *Atmos. Chem. Phys.* **2003**, *3*, 161.

(19) Wallington, T. J.; Hurley, M. D.; Ball, J. C.; Jenkin, M. E. *Chem. Phys. Lett.* **1993**, *211*, 41.

(20) Jenkin, M. E.; Hayman, G. D.; Wallington, T. J.; Hurley, M. D.; Ball, J. C.; Nielsen, O. J.; Ellermann, T. *J. Phys. Chem.* **1993**, *97*, 11712.

(21) Wallington, T. J.; Japar, S. M. *J. Atmos. Chem.* **1989**, *9*, 399.

(22) Sokolov, O.; Hurley, M. D.; Wallington, T. J.; Kaiser, E. W.; Platz, J.; Nielsen, O. J.; Berho, F.; Rayez, M. T.; Lesclaux, R. *J. Phys. Chem. A.* **1998**, *102*, 10671.

(23) Current recommendation of the IUPAC Subcommittee for Gas Kinetic Data Evaluation, available at http://www.iupac-kinetic.ch.cam.ac.uk/. Rate coefficients k_9, k_{13}, and k_{14} also in: Atkinson, R.; Baulch, D. L.; Cox, R. A.; Crowley, J. N.; Hampson, R. F.; Hynes, R. G.; Jenkin, M. E.; Rossi, M. J.; Troe, J. *Atmos. Chem. Phys.* **2006**, *6*, 3625.

(24) Volkamer, R.; Klotz, B.; Barnes, I.; Imamura, T.; Wirtz, K.; Washida, N.; Becker, K. H.; Platt, U. *Phys. Chem. Chem. Phys.* **2002**, *4*, 1598.

(25) Notario, A.; Mellouki, A.; Le Bras, G. *Int. J. Chem. Kinet.* **2000**, *32*, 105.

(26) Platz, J.; Nielsen, O. J.; Wallington, T. J.; Ball, J. C.; Hurley, M. D.; Straccia, A. M.; Schneider, W. F.; Sehested, J. *J. Phys. Chem. A.* **1998**, *102*, 7964.

(27) Sehested, J.; Møgelberg, T.; Wallington, T. J.; Kaiser, E. W.; Nielsen, O. J. *J. Phys. Chem.* **1996**, *100*, 17218.

(28) Wallington, T. J.; Hurley, M. D.; Haryanto, A. *Chem. Phys. Lett.* **2006**, *432*, 57.

(29) Vaghjiani, G. L.; Ravishankara, A. R. *J. Phys. Chem.* **1989**, *93*, 1948.

(30) Wallington, T. J.; Dagaut, P.; Liu, R.; Kurylo, M. J. *Int. J. Chem. Kinet.* **1988**, *20*, 177.

(31) Le Calvé, S.; Le Bras, G.; Mellouki, A. *J. Phys. Chem. A* **1997**, *101*, 5489.

(32) Jenkin, M. E.; Hayman, G. D. *Atmos. Environ.* **1999**, *33*, 1275.

JP908158W